Arab J Sci Eng
DOI 10.1007/s13369-014-1109-4

RESEARCH ARTICLE - EARTH SCIENCES

Close Range Photogrammetry Using Dense Epipolar Matching (DEM)

I. Zeroual · A. Liazid · P. Grussenmeyer

Received: 14 August 2012 / Accepted: 31 October 2013

Abstract This paper deals with the close numerical photogrammetry applications using several testing objects. The different steps of the metrological process are recalled and discussed according to the obtained results. To get effective geometrical information on objects, automation by stereo matching is needed for profit ability and homogeneity requirements. The qualitative and quantitative evaluation of the 3D accuracy of measurements and the analysis of the resulting dot cloud is done according to a known reference. This study proposes restitution for metrological requirements using the method of dense epipolar matching. Mappings quite redundant and distributed on the images, but also a denser reconstruction are preferable for the application of the surface reconstruction. The use of a digital reflex body CANON EOS 5D with focal of 20 and 28 mm enabled us to observe concretely the influence of the measurements accurately and the step to be planned for a metrology project.

Keywords Close range photogrammetry · Dense stereo matching · Calibration · Metrology

الخلاصة

تتعامل هذه الورقة العلمية مع تطبيقات التصوير الرقمي الختامية باستخدام عدة كائنات اختبار، حيث تم استدعاء الخطوات المختلفة لعملية القياس ومناقشتها وفقا للنتائج التي تم الحصول عليها. وللحصول على معلومات هندسية فعالة حول الكائنات، فهناك حاجة للأتمتة عن طريق تطابق الستيريو لقدرة الربح ومتطلبات التجانس. وتم التقييم النوعي والكمي للدقة ثلاثية الأبعاد للقياسات والتحليل لنقطة السحابة الناتجة وفقا لمرجعية معروفة. وتقترح هذه الدراسة تعويضا لمتطلبات القياس باستخدام طريقة مطابقة رؤية الستيريو الكثيفة (DEM). والتعيينات هي زائدة جدا وموزعة على الصور، ولكن أيضا إعادة بناء الكثافة هو أفضل لتطبيق إعادة بناء السطح. واستخدام الجسم العاكس الرقمي EOS 5D CANON مع تنسيق من 20 مم و 28 مم، مكننا من المراقبة بشكل ملموس ودقيق لتأثير القياسات بدقة والخطوة التي يجب أن يخطط لها لمشروع المقاييس.

1 Introduction

The objectives of this study devoted to metrology in close photogrammetry coupled with algebraic and numerical recent methods have allowed the improvement of multiple views treatment in photogrammetry. Based on those, the computer allows to perceive in three dimensions the scene observed and to establish measurements. Modeling through a mathematical method, then effective resolution by taking into consideration the errors of measurement related to the real world will be subject to analysis and discussions. The use of the unit beam as an approach of treatment allows talking about the epipolar geometry to attach one or more pairs of photography and to resolve the problem of the image dots correspondence. In a stereoscopic couple, the epipolar geometry informs us that for each dot observed in an image, it can be observed in another one only along one line, called "epipolar", and known, Fig. 1. Hence, several authors were interested with the quality standards and the accuracy study of measurement in close photogrammetry [1,2].

I. Zeroual
Faculty of Earth sciences, Oran University, El Mnaouer,
B.O. 1505, 3100 Oran, Algeria
e-mail: zeroual_ib@yahoo.fr

A. Liazid (✉)
LTE Laboratory, El Mnaouer, B.O. 1523,
31000 Oran, Algeria
e-mail: ab-liaz@hotmail.fr

P. Grussenmeyer
INSA Strasbourg, Group PAGE equips TRIO-LSIIT UMR 7005,
Strasbourg, France
e-mail: pierre.grussenmeyer@insa-strasbourg.fr

Published online: 01 May 2014

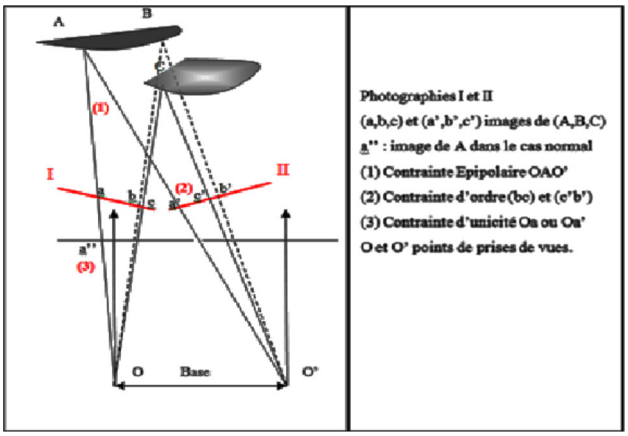

Fig. 1 Geometrical constraints in stereoscopy

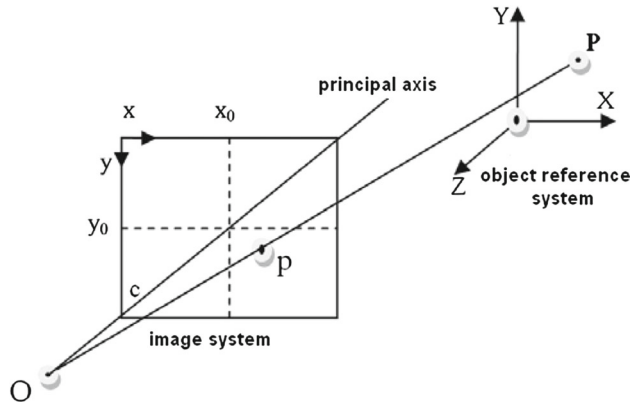

Fig. 2 Basic scheme for colinearity condition

The use of photogrammetry in industrial metrology field generates multiple problems. Indeed, there are various applications where the effectiveness of the photogrammetric methods remains to be proved [3–5]. We wish to use a sufficiently general tool of mapping able to consider images taken under conditions slightly different (position and orientation). The calibration implies the consideration of various rotations with nonparallel axes leading to very different images of the same scene [6]. It is illusive to hope for a perfect mapping process due to the geometrical nature of the constraints. In the vicinity of interesting points, it is important to have a rich enough signal allowing a good identification. The coded targets make it possible to reach this situation, but in a general way this approach is not exhaustive. In addition, the large varieties of deformation exclude the use of the stereo matching, which implies certain conditions of view catches. The stereoscopic parallax of a couple is a good indicator of geometrical configuration and improves the global treatment of 3D model calculation. The resolution of the metrology problem requires setting up auxiliary parameters. The use of a multi-scale approach can make positive improvements for measurement [7,8]. The SIFT (scale invariant feature transform) method performed by Lowe [9] is widely used for the mapping between images in photogrammetry and computer vision.

The recent developments in the industrial measurement using numerical photogrammetry cover a wide field of different challenges in terms of indicated accuracy, speed of measurement, automation, integration of process, and cost–time ratio. The accuracy and traceability checking by taking into consideration national and international standards is inevitable in industrial practice. System solutions could be divided into measurement of points, deformations and movements, 3D cuttings and discrete 3D surfaces. The recent and future developments focus on more robust dynamic applications, the integration of the systems in line productions, solutions of integration where the accuracy is higher for low costs [10].

2 Principle and Method

The three-dimensional world is projected in two bi-dimensional images; it is an application of a 3D space into a 2D space by reciprocity of the stereoscopy. For the multiple views [11], the principle is based on the dense stereo matching between images. The generalization of epipolar geometry concepts and the application of the invariants theory bring several solutions related to the applications of close photogrammetry [12]; orthophotographies, bi-ratio and rectification, monoimage restitution, etc…

The principle of the treatment method in photogrammetry is divided into two steps:

- Calibration of the photographic device (or several devices) and definition of the internal elements.
- Reconstitution and restitution of the object using the stereo matching principles like the DEM which is a method for locating a point by the intersection of two rays from two centers of perspective (Fig. 1).

2.1 Calibration

If the considered topic in this paper is focused on the influence of the metrology errors from a coded leveling (A0 format) which represents the reference points, the formulation of the problem taking into account these errors alongside research areas widely invested [11]. Indeed, the formulation considering the capacity to estimate jointly the position of each view, the model structure and parameters of the cameras widely used in photogrammetry.

Requiring an approximate model of the leveling, the approach is compared of 3D calibration, but keeps an important advantage to integrate internal parameters vector of complex camera ready to take into consideration deformations of important images (Fig. 2). Calibration's technics include the consideration of image deformations were introduced by the

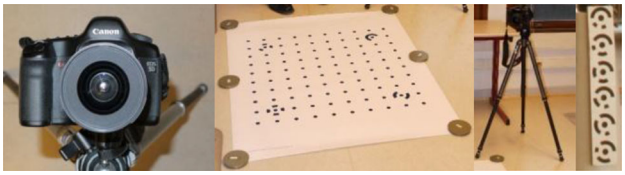

Fig. 3 Reflex Canon device, A0 calibration target, tripod and targets

photogrammetry specialists using the not calibrated cameras [6].

It is useful to point out the need for defining the internal elements of the camera. The principal distance, the image format and the distortions are as many factors to be calculated for the project. In metrology, the calibration is based on image observations with coded targets. The equipment system is composed of a camera and a 2D leveling containing 100 target points allowing internal elements calculation based on several images (Fig. 3). The calibration process optimization is based on the beams method [13,14], (Fig. 4).

The distortion formulation is the one defined by Brown [15] and it is proper to remind that in this work, only radial and tangential distortions are taken into consideration:

$$\begin{aligned} \Delta_{xr} &= x'(K_0 r^2 + K_2 r^4 + K_3 r^6) \\ \Delta_{yr} &= y'(K_1 r^2 + K_2 r^4 + K_3 r^6) \\ \Delta_{xt} &= P_1\left[r^2 + 2x'^2\right] + 2P_2 x' y' \\ \Delta_{yt} &= P_2\left[r^2 + 2y'^2\right] + 2P_1 x' y' \end{aligned} \tag{1}$$

where:

- K_1, K_2, K_3 are the parameters of polynomial model of radial distortion,
- P_1, P_2 are the parameters of polynomial model of tangential distortion,
- $r^2 = (x' - x_0)^2 + (y' - y_0)^2$; Radial distance calculated from the principal point.

The calibration parameters are thus calculated and expressed with the coefficients K_1, K_2, K_3, P_1, P_2, the principal distance value and the principal point coordinates. The interest is to obtain a corrected image of the various distortions.

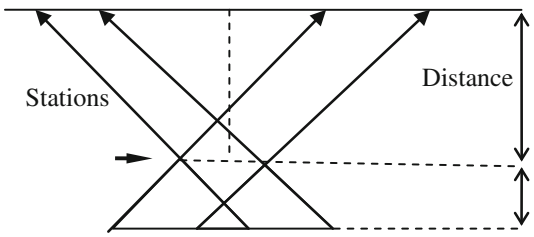

Fig. 4 Acquisition scheme for the DEM

2.2 Restitution Methods

In numerical photogrammetry, the restitution or reconstruction in 3D space is based on the generation of dot cloud. The dense methods in stereoscopy are limited to calibrated devices and very close points of view [10,16]. The applications of modeling and visualization require dense or almost dense reconstruction. The calculation of the dense mapping begins with pairing from some points of interests as the targets to refine the orientation while detecting and eliminating the aberrant points. The automatic orientation is based on the junction points connecting various photographies.

The stereoscopy relations in photogrammetry enable us to calculate the 3D position of a point corresponding to the homologous points. According to the constraints, the pairing solutions can be multiple or non-existent (noise ratio). So, it becomes necessary to apply constraints to the problem of the stereo matching to converge towards an existing, single and stable solution relating to the object. The acquisition to perform the model 3D is subject to a group of error sources which depend mainly on:

- Intrinsic camera parameters, and particularly the optical distortions which transform the lines (also the epipolar) into curves (Fig. 1).
- Position and orientation of the cameras, which differ from the normal case.
- Ratio R (base/distance), covering of the images, and existence of the objects on the images.

The ratio R must be optimized during the acquisition of the photography's, the intrinsic parameters are determined during the calibration of the device. The distortions and the deviations according to the normal case are corrected by epipolar rectification (creation of two virtual ideal cameras reported to the normal case). The resemblance between the intensities in the images for the homologous point's m and m' allows the calculation of the stereo matching between images. The following formulation allows expressing this function [17,18]:

$$m\,[x,\ y,\ I(x,\ y)] \Leftrightarrow m'\left[x',\ y',\ I'(x',\ y')\right] \tag{2}$$

Firstly, we studied the response of this technique to the needs of the 3D reconstruction. The elaborate criteria are based on:

- Geometry: fine detail and accuracy of the oriented model;
- The qualitative and quantitative rates allowing the analysis of the reconstruction.

Secondly, the technique currently used for statements and metrology measures may be subject to comparison with data objects. The external elements of the beams are calculated and analyzed according to the real situation of catch's views.

3 The Measuring System

The main device in close photogrammetry system is based on the cameras technology. The choice of the suitable device is based on accuracy, resolution, acquisition speed, synchronization, data size, spectral information, field of vision, image scale, numerical interfaces and cost. Nowadays, the variety of the cameras and video cameras available for image acquisition is enormous. Based on CCD and CMOS technology, the digital devices are available with very high resolution (>60 Mpixels), very high performance, size pixel variable between 1.4 and 15 μm, with different formats. For our experiments, we use a camera EOS 5D to analyze its metrological possibilities.

The photo modeler measurement system of EOS Systems is used for the photogrammetric measurements and treatments. The computing process is between orientation, determination of the external parameters and installation of an additional process (constraints) allowing the improvement of the restitution or the 3D model accuracy. The generation of a 3D model is based on a pair or a group of views distributed in a homogeneous manner relatively to the object. A set of basic geometrical forms (cylinder, cone), allows reconstructing the simple parts of the object. The creation of the group of dots allows a higher density and a choice of the 3D method modeling of the object. According to the theoretical principles, the working procedure of the professionals remains subject to errors in practical operations of measurements. The time of taking view as well as the environment surroundings, the resolution and the geometrical position of the images are a non-negligible set to analyze the photogrammetric treatment quality Table 1. Therefore, the calibration remains a necessary stage in the quality step. The experiment and the material used for these operations are summarized as follows:

- Photo modeler version 5.2 and photo modeler scanner version 7.
- Canon EOS 5D devices equipped with camera objective of 20 and 28 mm,
- Target calibration 2D (100 points of reference),
- Circular targets photo modeler 12 bits distributed on objects.
- Scanner 3D Trimble GX.

Table 1 Characteristics of taking views system

Description	Canon EOS 5D
Size in mm	35.8 × 23.9
Size in pixels	4,368 × 2,918
Image ratio	3/2
Sensibility	ISO 100–1,600
Sensor type	CMOS
Objectives	20 and 28 mm
Shutter speed	1″/8,000–30″

Our experience uses three tests defined according to the size, the distance and the complexity of the object. These tests are characterized by the parameters summarized in the Table 2.

The steps of determining the object are applied to the first test. The acquisition with the Laser Trimble GX scanner and coordinate measurements using Real Works 6.5 allowed the calculation of the 102 dots (17 blocks with 6 targets). This technology uses the measurement of the travel time of a laser light beam between the scanner and the point on the surface of the measured object (Fig. 5).

The time t of the laser beam path (propagating at the light velocity v) between the scanner and the point on the surface of the object is considered in the distance calculation formula given by the equation: $D = v * t/2$. Due to the high light velocity ($\approx 3.10^8$ m/s), the accuracy is almost independent of the measured distance. The measure accuracy is limited to 5 mm on the object (with the Trimble GX scanner at January 2011) and remains sufficient to validate our experience because the data quantification and their coherence by taking into consideration the reported treatment are the essential aspects of our study. The distance station/target is of 5 m. Concerning the two other tests, the distances between targets are enough to orient the model. The setting up of an acquisition scheme based on close couples to the normal case is desirable for the DEM.

4 Results and Discussion

The reliability of the process and its impact to satisfy a good reconstruction implies the consideration of several parameters.

Table 2 Experimental test parameters

Experience	Volume	Distance (m)	Recovery (%)
Test 1 (laboratory)	10 m^3 × 10 m^3 × 3.5 m^3	5	60–80
Test 2 (wild B9)	1.5 m^3	1	>70
Test 3 (mechanical object)	64 dm^3	0.5	>70

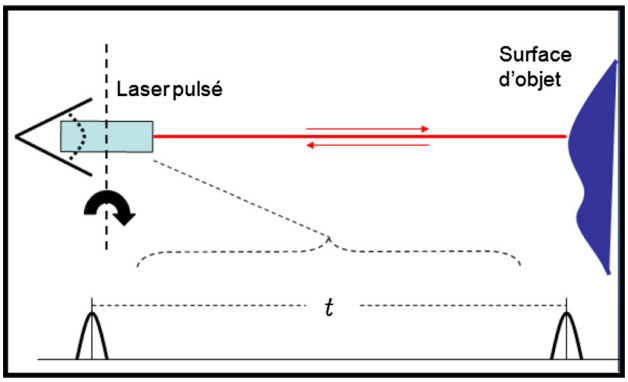

Fig. 5 Principle of distance measurement by measuring the travel time of a laser light

4.1 Calibration and Orientation

The A0 calibration target, including 100 dots has served to calibrate the Canon EOS 5D device. Figure 6 illustrates the result of the calibration on the 100 reference dots. For this operation, the after calculation residues are of 0.5 pixel (Fig. 6).

The parameters resulting from calibration calculations are summarized in the Table 3. For each camera; two calibrations tests are performed to evaluate the conditions impact on data acquisition. Very small deviations are observed according to the used images.

The distortion curves corresponding to the two objectives (20–28 mm) for the Canon EOS 5D devices are represented in Figs. 7 and 8, which express the radial distortion (with considering the other distortions negligible). The parame-

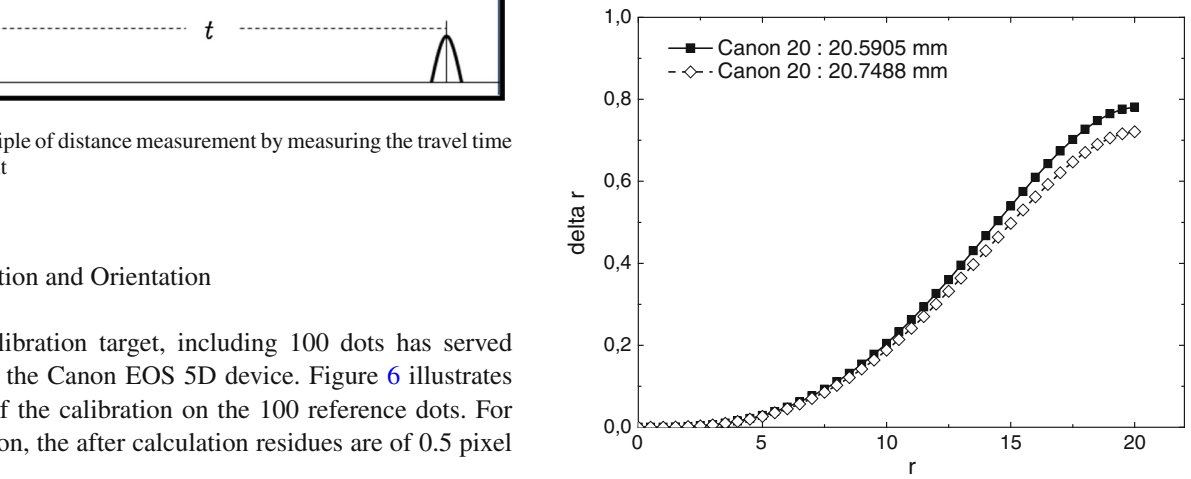

Fig. 7 Distortion curves (objective of 20 mm)

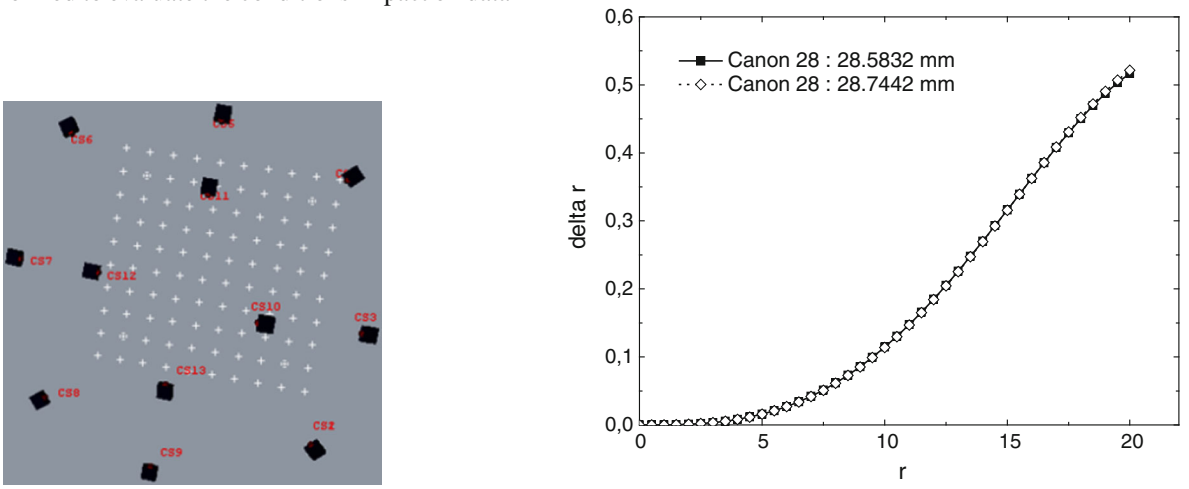

Fig. 8 Distortion curve (objective of 28 mm)

Fig. 6 Reference stations and targets configuration

Table 3 Results of the internal elements of the calibration

Internal parameter	Camera 20 mm		Camera 28 mm	
Focal (mm)	20.591	20.749	28.583	28.744
Format (mm)	35.792 × 23.927	35.808 × 23.927	35.891 × 23.927	35.851 × 23.927
Principal dot (mm)	17.951–11.963	17.995–11.963	17.857–12.107	17.916–11.963
K_1	2.1×10^{-4}	2.21×10^{-4}	1.31×10^{-4}	1.30×10^{-4}
K_2	3.57×10^{-7}	3.27×10^{-7}	-1.659×10^{-7}	-1.62×10^{-7}
K_3	0	0	0	0
$P_1 - P_2$	0	0	1.07×10^{-5}; 0	1.071×10^{-5}; 0

Table 4 Differences obtained on the calibration target

Calibration test	SD in X direction (mm)	SD in Y direction (mm)	SD in Y direction (mm)	SD on residues (pixels)
Canon 20 mm	0.3 E−03	1.2 E−03	0.9 E−03	0.025
Canon 28 mm	1.2 E−03	0.7 E−03	1.1 E−03	0.047

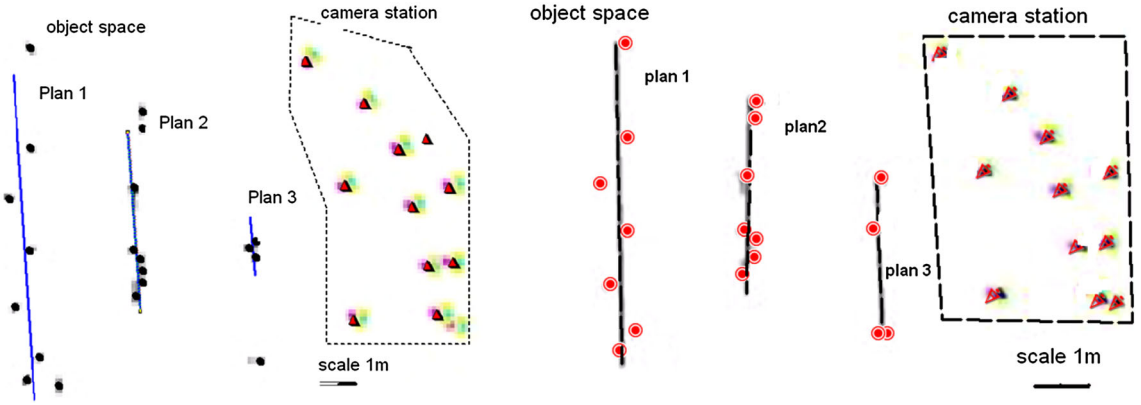

Fig. 9 Global setting camera/target. **a** Canon EOS 20 mm. **b** Canon EOS 28 mm

ters P_1 and P_2 provide a maximum correction of 0.3 μm (=0.01pixel).

The entirely calculation of the 3D model with the beams provides the results registered in the Table 4:

The acquisition process includes the catches of views for the calibration and the catches of views for the restitution. In the first test, the experience performed made at the laboratory level uses 17 patterns representing 102 coded targets with 12 bits. The space, of the considered experience is defined with a volume of 10 m^3 × 10 m^3 × 3.5 m^3 with three plans containing the targets (Fig. 9). The observation stations are located on very close points, the surface detection is observed with deviation of ±5 mm. Figure 9a and b present this aspect according to the real object (position, dimension, shape). After correction of images, these figures express the shape and dimension of the returned points. The results show a slight difference in the position of the returned target. Table 5 gives a value of the standard deviation obtained by the calculation of the 3D process. The result is oriented towards the use of camera with a long focal length (28 > 20). So, it is noticed that the total configuration is well preserved.

The restitution is started by DEM after validating the orientations of distortions on corrected images. The deviation observed at the edges of the corrected image reached a maximum value of 0.35 mm. The deviation is with a flat shape defined by a black band on the image limits. The average differences on the support dots are summarized in Table 5. It is noticed that the component value of the residual space difference agrees the global accuracy of the measurement system

Table 5 Deviations on support dots

Test	Deviation (mm)	Deviation (mm)	Deviation Z(mm)	Standard deviation on residues (pixels)
Canon 20 mm	3.1	3.2	3.2	0.100
Canon 28 mm	1.8	2.1	5.6	0.090

Table 6 Differences between measured and calculated distances

Station number	St2–St3	St3–St4	St4–St5	St5–St6
Measured distance (mm)	1,450	1,180	1,230	1,175
Calculated distance (mm)	1,449	1,181	1,229	1,176
Standard deviation (mm)	±1	±1	±1	±1

(≈5 mm) calculated on the basis of 103 dots. The standard deviation of residues is determined with a sample of 400 dots spread out between connection dots and support dots.

The difference between the calculated distances by the photogrammetric system and those measured between stations of view catches are summarized in Table 6. This control allows the validation of the external orientation, notably the position of the stations as external parameters.

The observed deviations are due to approximate measurements and uncertainty of the reference frame established during the referencing operation. The choice of the reference points according to the images and the geometrical constraints installation allows the improvement of the accu-

Table 7 Refinement of the 3D calculation for the two tests

Test	Deviation x (mm)	Deviation y (mm)	Deviation z (mm)
Canon 20 mm	0.3	0.3	1
Canon 28 mm	0.2	0.2	0.3

racy and calculation of the 3D model. The aggregate Table 7 of the differences shows a precision of 2×10^{-4} m on the positioning of the points. The calculation of the 3D model is refined using support dots which give a better quality (a good pointed) characterized by a good intersection of the rays and intersection angles.

The global configuration of the whole entities of a scene allows answering effectively on the quality of the new 3D dots. The parameters analysis of the global treatment (calibration, orientation and restitution) gives further information on the relative accuracy which is 0.001 % of the object size. The space stereo matching between the image, the object and its reconstruction in 3D could be estimated using the Jacobean matrix in the calculation process of the models in 3D dimensions [3].

4.2 The Restitution

It is obvious that for the catches of views with a focal distance of 20 mm, the object is in a closer situation compared to other focal distances 28 mm (Fig. 10). In the optical processes, measurement is faded whatever is the system used; indeed, the conditions of illumination, the elements position of the subject and the cameras, the catch of view and the various adjustments allow to obtain a good quality image. In photogrammetry, the reconstruction is based on the images correspondence and the homologous ray's intersection. Compared to the traditional process, it is judicious to analyze the ratio base/distance to extract an ideal position from the stations of catches of views. The general diagram for the photogrammetric treatment is represented in the Fig. 11.

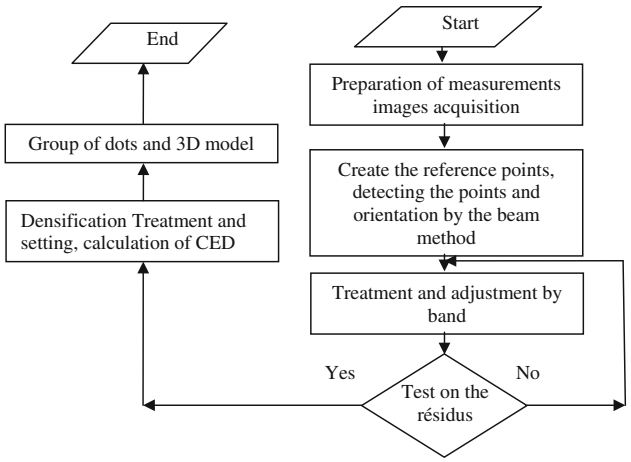

Fig. 11 Diagram of the treatment process

4.2.1 The Matching for Relative Orientation

The multi-view stereo matching is carried out automatically using the orientation module without taking into consideration the subject coordinates. After segmentation of the generated file, the error classes in pixels defined for the three tests encourage this way to approach the restitution. Globally, the correspondence error is lower than 1 pixel. The following tables illustrate the results of this calculation for the three tests. The number of paired dots expresses a good stereo matching for relative orientation according to the error classes between 0 and 3 pixels. The aberrant or false values are rejected.

4.2.2 The Restitution

The observed objects are illustrated in Figs. 12, 13, 14. The generation of the points cloud remains essential because it allows setting optimal conditions for the catches of views, including the ratio base/distance. Knowing that DEM method is based on a calculation by couple of beams, the algorithm has $(n^2 - n)/2$ possibilities allowing the densification [19]. A ratio between 0.1 and 0.3 for the calculation of intersections

Fig. 10 Scene acquisition with the Trimble GX scanner

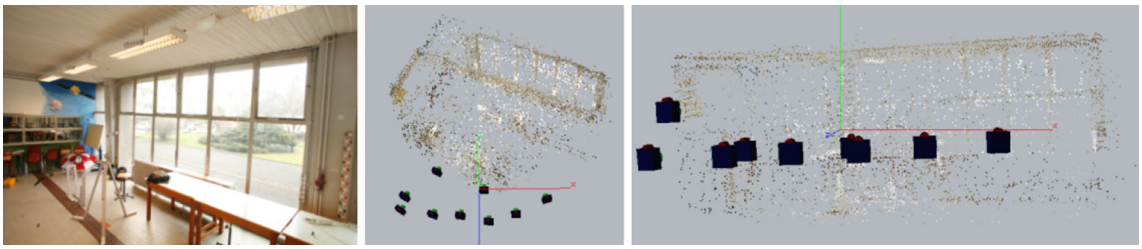

Fig. 12 3D calculation result. Case of Test 1 (labo-topo)

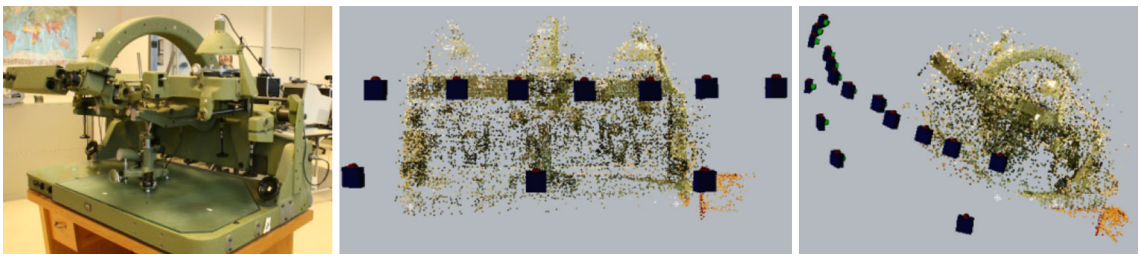

Fig. 13 3D calculation result. Case of Test 2 (wild B9)

Fig. 14 Test result. Case of Test 3 (mechanical part)

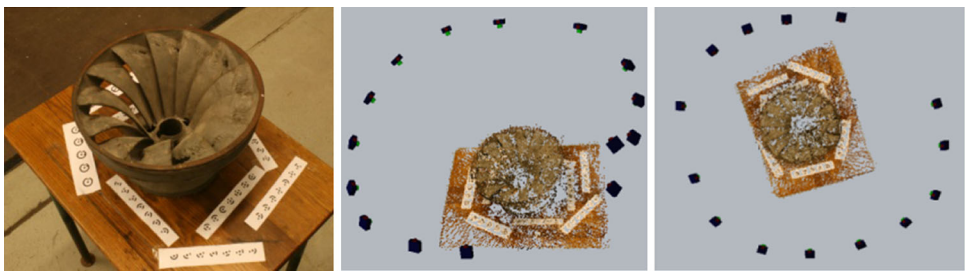

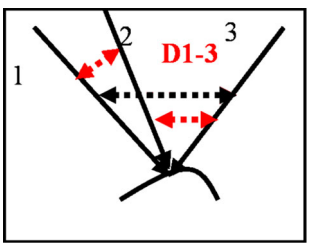

Fig. 15 Homologous ray's intersection from many photography

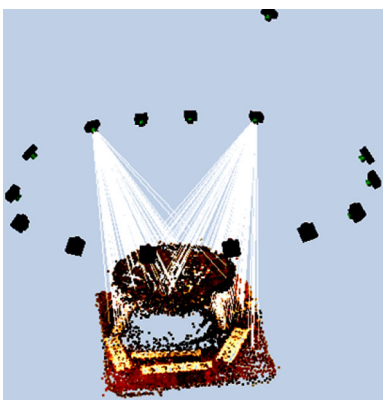

Fig. 16 Homologous ray's intersection for the restituted piece

between matched dots by the DEM is recommended [18]. Table 11 summarizes the results for values of the B/H ratio ranging between 0.1 and 0.3. The angles of the intersected rays are variable and inform us on the determination of the stereoscopic dot. It is noticed that there is a strong stereo matching between intersection and angular value.

Point's clouds generated are dependent on all treatments applied upstream namely the internal and external orientations. The comparison with auxiliary data (external and independent) allows certifying the process of measurement and calculation. Actually, accuracy measurements are produced if independent data of dot support and check dots are available in object space. A complete model allowing the correction of these deformations and ensuring the quality of treatments in photogrammetry can be presented only if the aggregation of the parameters could be modeled [16]. There are several indicators allowing evaluating the quality of a good restitution. The value of space intersection (tightness

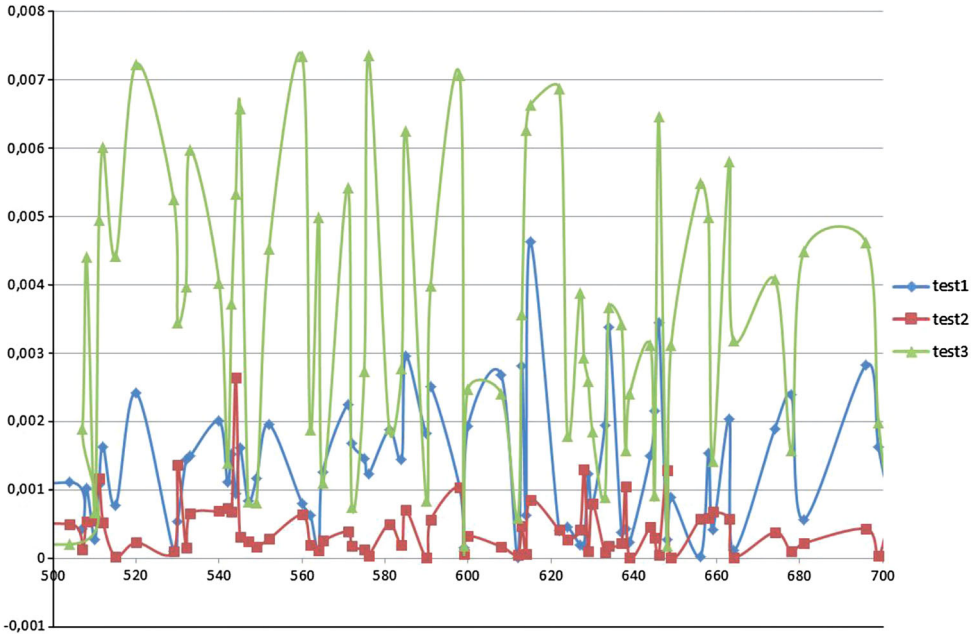

Fig. 17 Homologous ray's intersection for each project

index) is an answer to these problems by applying a topological calculation detecting the dot according to the position of the homologous rays (Figs. 15, 16). This value used to indicate the accuracy of an Object Point's photo markings in conjunction with the accuracy of the camera station orientations (Fig. 17). 'Tightness' is displayed in a number of areas of which the most commonly used is the point table. The 3D position of an object point is computed by intersecting light rays from photographs. Due to measurement error, these light rays never intersect at a perfect point in 3D space. If we call the closest distance between any two light rays k and j used in the computation of point i as CDikj, define the largest CDikj value for any point i as LEi, and we call the approximate project size (as entered in the project information dialog) as PS. Then the tightness value is a percentage computed as:

LEi = maximum (CDikj for all k and j)
Tightness of point i = LEi / PS × 100
Example of a point number 10 appearing on three photos:
CD10, 1,2 = 0.1 cm
CD10, 1,3 = 0.2 cm
CD10, 2,3 = 1.0 cm
Therefore, LE10 = 1.0 cm
PS = 20 m

Therefore, tightness for point 10 = 0.01 m/20 m × 100 = 0.05 %

In practice, neither marking nor the calibration and the orientation are perfect. This implies that the homologous rays do not intersect but they define in the vicinity of the considered dot a metric distance allowing the choice of the most probable dot calculated on the basis of a maximum distance between rays. Because of measurement error, these rays never intersect in a perfect point in the 3D space. Figure 16 shows the relative accuracy of the intersection of the homologous rays for the three tests, it is expressed according to the size of the object (d). According to current work in photogrammetry, an intersection ratio of 0.1 %d corresponds to a good restitution. For work with high accuracy degree, this ratio must be lower than 0.01 % [10,20]. Results obtained on bulky objects

Table 8 Errors repartition on image coordinates for Test 2

Test 2 (wild-B9)	Number of points	Presence rate (%)
Class [0–1 pixel]	379	59.2
Class [1–2 pixels]	202	31.6
Class [2–3 pixels]	59	9.2

Table 9 Errors repartition on image coordinates for Test 1

Test 1 (labo-topo)	Number of points	Presence rate (%)
Class [0,1 pixel]	174	50
Class [1,2 pixels]	133	38.2
Class [2,3 pixels]	41	11.8

Table 10 Errors repartition on image coordinates for Test 3

Test 3 (piece)	Number of points	Presence rate (%)
Class [0,1 pixel]	248	50
Class [1,2 pixels]	170	34.2
Class [2,3 pixels]	78	15.8

Table 11 Result of treatment for the three tests

Project	Number of couples	Number of dots	Absolute and relative accuracy on the homologous rays intersection	Angle of dots intersected in degree
Test 1 : labotopo	26	8,009	0.00051–0.000005	1.866°–81.540°
			2.55–0.025 (mm)	
Test 2 : wild B9	47	17,851	0.005–0.00001	4.476°–89.300°
			5–0.001 (mm)	
Test 3 : mechanical part	21	19,884	0.0085–0.000019	7.070°–89.960°
			1.91–0.004 (mm)	

Bold values indicate the error range of the intersection of homologous beams

($\approx$100 m^3) allow certifying the recent developments of the method in industrial metrology [21,22].The contribution of auxiliary data and the indexing in the treatments of geometrical primitives is an alternative for the 3D reconstruction and allows obtaining a good accuracy [23].

5 Conclusion

Photogrammetric metrology integrates the data of the object space and those related to the image. Research of a unique and reliable solution is not easy to achieve. The choice of camera, stations and targets to reach this solution is necessary. The contribution of the DEM is certainly with a great importance for the restitution of 3D models. This technique largely used in the closer field in photogrammetry can be very appreciable in industrial metrology (on objects of intermediate size). The stereo matching is proved to be geometrically very powerful because it is independent of the object size and it allows offering models resulting from adjustment by band or beams giving place to a reliable total configuration from the object. The treatment for metrology is validated with each phase:

- The study of the calibration and the obtained results were satisfactory with the use of polynomial parameters K1, K2, P1, and P2. This study has set the conditions for adequate treatment.
- The photography's orientation and the cameras positioning allowed us to optimize the number of stations shooting. The long focal rooms are recommended for close objects using the DEM method. The B/H (base isolation) <0.3 is a criterion indicating good results. Tables 4, 5, 6 express this aspect.
- The 3D restitution of the studied examples shows through Tables 8, 9, 10, 11 the achieved accuracy in the reconstruction of test objects. The relevance of measurement results requires a good intersection ray's counterparts.

The latest innovations in image correlation algorithms allow simultaneously the combination of several photographs (more than two) to improve the geometric constraint for point cloud as faithful as possible to reality. Photogrammetry is not intended to replace the laser scanning. However, it can be seen as a means of effective complement. For many projects, the use of a multi-technique is an optimal solution to optimize both time and quality of work.

Acknowledgments This work was achieved at INSA of Strasbourg. Our thanks are addressed to the members of the PAGE group, in particular Samuel Guillemin for his availability during the experiments.

References

1. Mikhail, E.M.; Bethel, J.S.; McGlone, J.C.: Introduction to modern photogrammetry. Wiley, New York (2001)
2. Fryer, J.; Mitchell, H.; Chandler, J. (eds.): Applications of 3D measurement from images. Whittles, Scotland (2007)
3. Förstner, W.: Manual of photogrammetry, 5th edn. ASPRS, chap. 11, quality of 3D points, pp. 800–804 (2004)
4. Sanz-Ablanedo, E.; Rodríguez-Pérez, J.R.; Arias-Sánchez, P.; Armesto, J.: Metric potential of a 3D measurement system based on digital compact camera. Sensors **9**, 4178–4194 (2009)
5. Eos Systems Inc., Photo Modeler Pro User's Manual, Version 7 (2010) http://www.photomodeler.com
6. Luhmann, T.; Robson, S.; Kyle, S.; Harley, I.: Close range photogrammetry: principles, methods and applications, p 528. Whittles, Scotland (2006)
7. Förstner, W.: A feature based correspondence algorithm for image matching. Int. Arch. Photogramm. **26-3/3**, 150–166 (1986)
8. Kalantari, M.; Jung, F.: Estimation automatique de l'orientation relative en imagerie terrestre. Revue XYZ, n°114, pp. 59–63 (2008)
9. Lowe, D.G.: Distinctive image features from scale invariant keypoints. Int. J. Comput. Vis. **60**(2), 91–110 (2004)
10. Luhmann, T.: Close range photogrammetry for industrial applications. ISPRS J. Photogramm. Remote Sens. **65**(6), 558–569 (2010)
11. Hartley, R.; Zisserman, A.: Multiple view geometry in computer vision. Cambridge University Press, Cambridge (2004)
12. Grussenmeyer, P.; Al Khalil, O.: Solutions for exterior orientation in photogrammetry, a review. Photogramm. Rec. Int. J. Photogramm. **17**(100), 615–634 (2002)
13. Zeroual, I.; Liazid, A.: Use of DLT in photogrammetric Metrology—ISPRS commission V, Corfu (2002)
14. Zeroual, I.; Liazid, A.: Expérimentation de la Transformation Linéaire Directe pour différentes applications en photogrammétrie. Revue XYZ, N°106, pp. 35–40 (2006)

15. Brown, D.C.: Close range camera calibration. Photogramm. Eng. **37**(8), 855–866 (1971)
16. Rieke-Zapp, D.H.: Peipe, J.: Performance evaluation of a 33 megapixel alpha 12 medium format camera for digital close range photogrammetry. In: Proceedings of the ISPRS Commission V Symposium Image Engineering and Vision Metrology, Dresden (2006)
17. Kasser, M.; Egels, Y.: Digital photogrammetry. Taylor and Francis, London (2001)
18. Hullo, J.F.: Acquisition de nuages de points denses par photogrammétrie terrestre. Revue XYZ n°122, pp. 19–26 (2010)
19. Barazzetti, L.; Remondino, F.; Scaioni, M.: Automation in 3D reconstruction: results on different kinds of close-range blocks. International Archives of Photogrammetry, Remote Sensing and Spatial Information Sciences, Vol. XXXVIII, Part 5, Commission V Symposium, Newcastle upon Tyne, pp. 55–61 (2010)
20. Fraser, C.; Cronk, S.: A hybrid measurement approach for close range photogrammetry. ISPRS J. Photogramm. Remote Sens. **64**(3), 328–333 (2009)
21. Ozbek, M.; Rixen, D.J.; Erne, O.; Sanow, G.: Feasibility of monitoring large wind turbines using photogrammetry. Energy **35**, 4802–4811 (2010) [Elsevier]
22. Arias, P.; Ordonez, C.; Lorenzo, H.; Herraez, J.; Armesto, J.: Low cost documentation of traditional agro-industrial buildings by close range photogrammetry. Build. Environ. **42**, 1817–1827 (2007) [Elsevier]
23. Jian-dong, Z.; Li-yan, Z.; Xiao-yu, D.; Zhi-an, D.: 3D curve structure reconstruction from a sparse set of unordered images. Comput. Ind. **60**(2), 126–134 (2009)